Research on Engineering Structures & Materials
www.jresm.org
MIM Research Group

Research Article

Experimental investigations on the corrosion behavior of Al–Mg/B_4C composites synthesized via powder metallurgy

Enas Khudhair [1,a], Asraa T. Nasser [*,2,b], Balsam M. Shaker [3,c], Saraa M. Mohammad [3,d]

[1]*Department of Technical Power Mechanics, Technical Engineering college / Najaf, Al-Furat Al-Awsat Technical University (ATU), Najaf, Iraq*
[2]*Chemical Engineering Department, Faculty of Engineering, University of Kufa, Iraq*
[3]*Department of Construction and Projects, Mustansiriyah University, Baghdad, Iraq*

Article Info

Article History:

Received 30 May 2026
Accepted 03 Aug 2026

Keywords:

Aluminum–magnesium alloy;
Boron carbide;
Powder metallurgy;
Corrosion;
Hardness;
Sodium chloride

Abstract

The goal of this project was to investigate the microstructure, hardness as well as corrosion behavior of Al - 4% Mg metal matrix composites containing boron carbide (B_4C) particles at different weight fractions (3, 6, and 9 wt.%). Composites were produced through powder metallurgy by compacting, sintering and characterizing using scanning electron microscopy (SEM), X-ray diffraction (XRD), hardness testing along with potentiodynamic polarization testing in 3.5% sodium chloride solution. The findings demonstrated that when sintered at 560 degrees Celsius (°C), particles of boron carbide dispersed evenly inside the Al-Mg matrix with low levels of porosity. Increasing the B_4C content improved hardness up to an optimal fraction of 6 wt.%; however, particle agglomeration at higher weight fractions reduced strengthening efficiency. Potentiodynamic polarization tests indicated that corrosion resistance was greater due to boron carbide particles up to a level of 6 % by weight as evidenced via lower corrosion current densities and reduced tendency to pitting, which was attributed to the barrier effect from ceramic reinforcement. At 9% by weight boron carbide, increasing agglomeration, microstructural defects and susceptibility to localized corrosion resulted from addition of boron carbide. The findings indicate that an optimum amount of boron carbide is necessary to optimize mechanical strength while providing the adequate levels of corrosion resistance; therefore, suggesting that the Al–4Mg–6B_4C composite is well-suited for marine and aerospace applications.

1. Introduction

Metal matrix composites (MMCs) combine a metallic matrix with a reinforcing material to produce enhanced physical, thermal, and mechanical properties. The increasing need for greater strength and higher levels of resistance to corrosion has made these composites increasingly popular in today's manufacturing industry. Due to their properties including higher stiffness, ability to withstand high temperatures, better resistance to wear, and lower thermal expansion, MMCs are widely used in a number of different markets such as aerospace, electronics, and marine applications. The methods of making all the composite materials are different depending on the type of reinforcement being used (for example, compo casting [1], Liquid Phase Infiltration [2], Squeeze Casting, Spray Co-Deposition [3]). There are many difficulties associated with the casting of composites including those reinforcements may not be evenly distributed in the matrix, the matrix and reinforcements may have a difficult time interacting at elevated temperature, and an irregularly formed matrix structure results in inconsistencies in bulk properties of the composite

*Corresponding author: esraat.alabass@uokufa.edu.iq
[a]orcid.org/0009-0006-5801-4159; [b]orcid.org/0009-0007-2876-3180; [c]orcid.org/0009-0005-8391-8048
[d]orcid.org/0009-0002-7674-2150
DOI: http://dx.doi.org/10.17515/resm2026-1720ma0530rs

materials [4,5]. These drawbacks underscore the significance of implementing powder metallurgy (PM) as a viable technique for composite manufacturing. Particulate reinforced composites fabricated through PM exhibit superior properties and improved metal working characteristics, making it a well-defined approach for manufacturing composite materials [1]. MMCs are widely applied in engineering industries because of their superior mechanical, thermal, and corrosion resistance properties. Aluminum-based alloys, in particular, are highly favored for their low density, excellent corrosion resistance, and machinability. The incorporation of alloying metals like magnesium promotes precipitation hardening and increases strength. Notwithstanding these benefits, Al–Mg alloys are susceptible to localized corrosion in hostile chloride conditions. The integration of ceramic reinforcements into aluminum alloys enhances hardness, wear resistance, and, in certain instances, corrosion resistance. Boron carbide (B_4C) is notable among these reinforcements for its exceptional hardness, low density, as well as robust chemical stability. Powder metallurgy (PM) offers a dependable technique for fabricating aluminum-based composites with uniform dispersion of ceramic particles, circumventing numerous casting-related complications such as segregation and porosity. Kumar et al. (2022) examined the electrochemical corrosion characteristics of boron carbide (B_4C) ceramic-reinforced Al-Mg-Si matrix composites in diverse aqueous conditions. The investigations demonstrated that the corrosion resistance of Al-Mg-Si composites is superior in NaCl medium, attributed to a smaller negative corrosion potential, elevated charge transfer resistance (Rct), and diminished double-layer capacitance (Cdl) relative to other media. The SEM morphology indicates that B_4C ceramics improve corrosion resistance by creating a protective barrier layer of OH- and Cl- deposits in the composite and unreinforced alloy, respectively [6]. Rahmani et al. manufactured and assessed the mechanical as well as wear characteristics of a magnesium metal matrix composite reinforced with 0, 1.5, 3, 5, and 10 vol.% B_4C micro-particles. The findings indicate that the hardness of SHB as well as DH samples is 20.2% and 5.7% greater than that of the QS specimen, respectively. The wear rate and mass loss of Mg−10.0%B_4C samples produced by SHB were found to be around 33% and 39% lower than those of the QS sample, respectively. The quasi-static compressive strengths of Mg−5.0%B_4C exhibit enhancements of 39%, 30%, and 29% for the SHB, DH, and QS samples, respectively, when compared to pure Mg. Moreover, it has been found that the dynamic compressive strength of samples is 51%–110% greater than their quasi-static value in relation to the B_4C concentration [7]. This study investigates the corrosion and hardness characteristics of Al–4Mg reinforced with several weight percentages of B_4C particles, with the objective of determining the optimal reinforcement ratio for structural applications in maritime and aerospace industries.

2. Experimental Work

2.1. Preparation of the Specimens

The investigations were made of the composite materials obtained with the powder metallurgy methods of the alloy reinforced with the Composites were fabricated with 3, 6, and 9 wt. % B_4C particles. Aluminum powder with 99.5% purity and an average particle size of 75 μm was mixed with 4 wt. % magnesium and reinforced with B_4C particles of average size <60 μm and 99% purity. Four compositions were prepared: Al–4Mg (base), Al–4Mg–3B_4C, Al–4Mg–6B_4C, and Al–4Mg–9B_4C. The following table shows the density and thermal properties of the utilized materials. These elementals and reinforcing powders were blended using a low-energy mixing process at 150 rpm for 45 minutes to attain a uniform dispersion of B_4C particles without causing excessive mechanical deformation of the ductile aluminum matrix. The compaction step was then conducted using a uniaxial pressure of about 100 MPa and employing standard lubrication of the die wall to prevent internal contamination of the powdered mix. The compaction profile attained through the above process is structurally capable of inducing localized plastic deformation of the Al particles to mechanically destroy the tenacious Al_2O_3 layer on its surface and generate uniform green compacts with a green density of about 83% of its theoretical maximum, yielding a total of 12 specimens (3 samples per formulation batch).

Table 1. Thermal Features and density of the materials

The material	Density in (kg/m^3)	The Thermal Conductivity in (W/m·K)	Specific Heat (J/kg·K)
Aluminum (Al)	2700	205	900
Magnesium (Mg)	1740	156	1020
Boron Carbide (B_4C)	2520	~35	750

2.2. Compaction and Sintering

Aluminum powder is amalgamated with magnesium powder and the reinforcement of boron carbide powder in meticulously regulated proportions. boron carbide was incorporated at three distinct levels, characterized by varying weight percentages of (3, 6, and 9 wt.%), and a fixed weight percentage of magnesium (4 wt.%) was added to the matrix alloys. Subsequently, the premixes underwent compaction utilizing a precision metal die with a diameter of 14 mm within a laboratory vertical unidirectional press possessing a capacity of 10 tons (~100 MPa), resulting in the formation of a green compact. Green compacts were sintered in vacuum at 560 °C for 3 hours and cooled in the furnace, as suggested by Jiang et al. [8]. This procedure facilitates the metallurgical adhesion of powder particulates, thereby cultivating the requisite physical and mechanical characteristics. The effective sintering of aluminum-based powders was realized within a vacuum milieu, as the sintering of aluminum powder presents considerable challenges due to the fact that aluminum oxide remains unreduced within the furnace atmosphere at conventional sintering temperatures. At the end of sintering, the temperature was cooled with the furnace. Finally, the obtained bars were turned into small specimens of 14 mm diameter and 25 mm length for use in the experiments. The temperature for sintering in vacuum was specifically kept at 560°C, which is well below the melting temperature of pure aluminum (660°C) and also the liquidus line of the Al-Mg system. The liquidus line ensures that solid-state sintering is done, without the risk of macrostructural distortions or complete melting of the matrix. The heat treatment process was controlled through a heating rate of 5°C/minute, as well as cooling of the specimens was done in the furnace slowly at 2-3°C/minute.

2.3. Characterization and Testing

2.3.1 Hardness Test

This measurement was carried out utilizing a Vickers Micro-hardness Tester in accordance with ASTM E384. The instrument was calibrated with a standard steel reference block prior to testing. Indentations were performed with a Vickers indenter (pyramidal diamond, four-sided) under applied loads of 100 gf and 500 gf with a dwell time of 15 seconds.

2.3.2 Corrosion Test

Potentiodynamic polarization was utilized alongside ASTM G59 [9] recommendations to make electrochemical corrosion measurements, while corrosion rates and current densities were found pursuant to ASTM G102 [10]. Prior to the measurements, the specimens had been ground and polished through the use of diamond abrasives and colloidal silica to achieve the mirror finish. The electrochemical measurements were performed via the Gamry potentiostat and Gamry Framework software. The working electrode was the composite specimen; the reference electrode was the saturated calomel electrode (SCE); and the auxiliary electrode was used in accordance with the experimental setup. The electrolyte consisted of the 3.5 wt.% NaCl solution. The open-circuit potential (OCP) was monitored during the first 150 s of the process and followed by a stabilization period of 150 seconds before initiating polarization. The potentiodynamic measurements were carried out in the range from −0.25 V to +0.25 V with a scan speed of 1 mV s^{-1}. The experiments were carried out at 25 ± 2 °C, and the values for corrosion potential (Ecorr), corrosion current density (Icorr), and corrosion rate were obtained through the Tafel extrapolation method on the basis of polarization curves.

2.3.3 Characterization of the Sintered Composite

The produced sintered specimens of Al-4Mg alloy and its composite were subjected to scanning electron microscope (SEM) before and after the electrochemical testing in 3.5% NaCl solution. A careful investigation was made for observing microstructure of samples. The phases present in the samples from various processing conditions were identified using X-ray diffraction (XRD) to determine the types of intermetallic formed in each metal matrix composite sample.

3. Results and Discussion

3.1. Microstructural Analysis

The microstructure of the prepared alloy and its composites sintered at 560°C for 3 hours was analyzed through a scanning electron microscope and shown in Figure 1, to identify the layout of B_4C particles within the Al-4Mg alloy matrix. It is evident from Figure 1 that the distribution of the particles manifests a nearly homogeneous characteristic for both the alloy and its composite constituents.

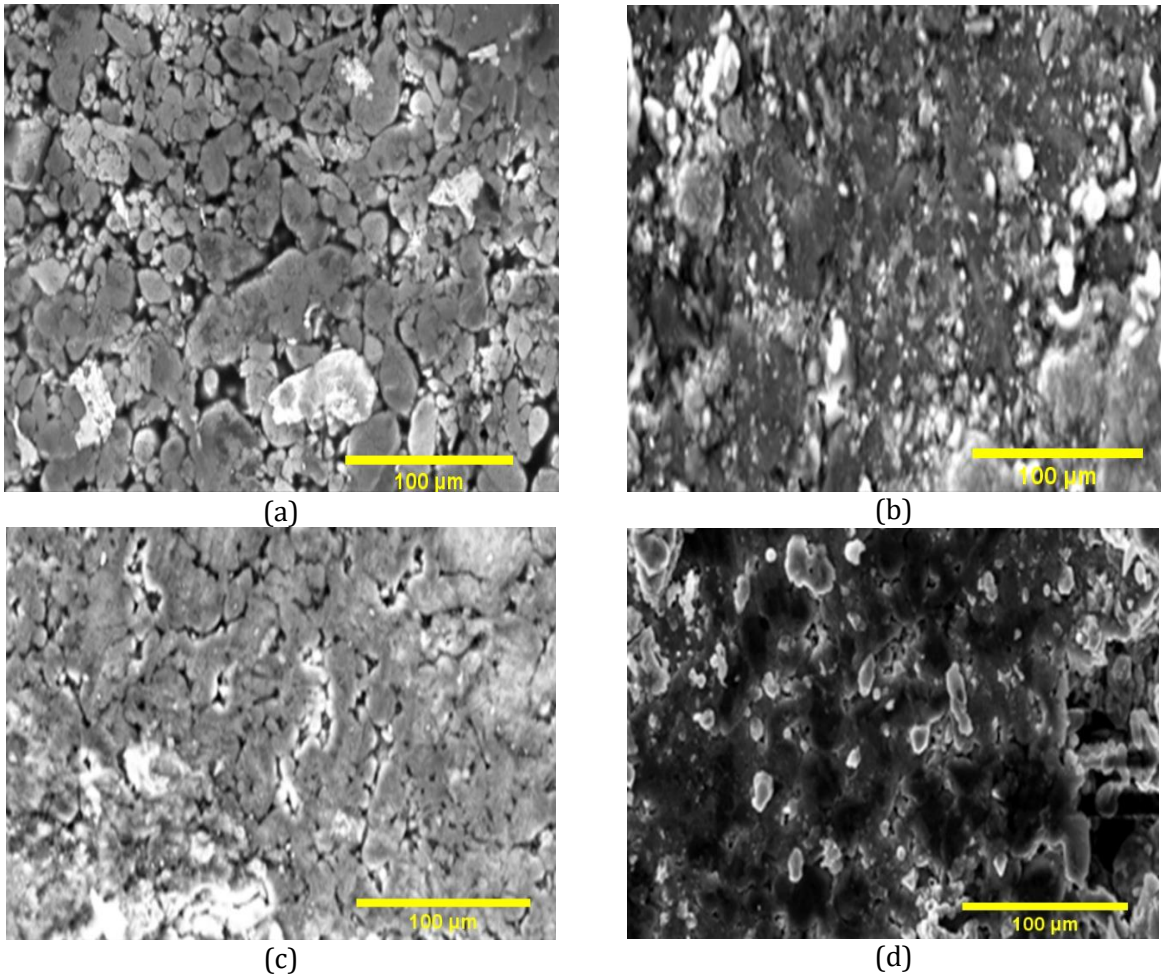

(a) (b) (c) (d)

Fig. 1. Microstructure of the produced Al-4%Mg-XB_4C alloy and its composite (a) 0% (b) 3% (c) 6% (d) 9%

It is expected that the powder metallurgy processing technique will yield a homogeneous distribution of microstructures due to the way powders were initially combined; this process will provide for a uniform structure in the final sintered product after sintering has taken place. Another key observation made from figure 1, concerns how well the actual sintering operation has performed. Based on the findings displayed in figure 1, it appears that at no time have major signs of any types of voids, fractures, surface defects and/or any other types of irregularities occurred, which provides evidence that the sintering operation was properly performed and fully completed, producing completely dense and solid composite materials. The micrograph indicates that

aluminum dendrites and aluminum intermetallic compounds with magnesium were all part of the overall microstructure. As B_4C is integrated into the alloy, the intermetallic phases exhibit a change in contrast from black to grey. The chemical composition of the intermetallic depends on the alloy composition as well as the cooling rate [11]. The alteration of the chemical composition of these intermetallic phases markedly affects the corrosion characteristics of the material [12]. Nevertheless, some residual micro-porosity is noted, likely attributable to the inadequate sintering temperature of 560 °C, which proved insufficient to facilitate the formation of a liquid phase during the process.

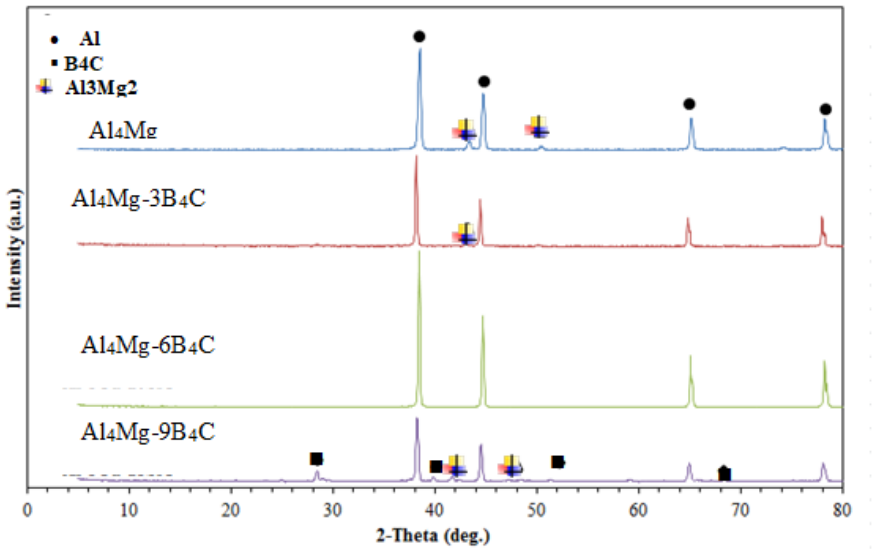

Fig. 2. XRD pattern of composites sintered at 560 °C for 3 hours of Al-4%Mg-XB_4C composites.

The different XRD patterns that originated from the preparation of the Al-4Mg-xB4C composite with different amounts of SiC particles (0, 3, 6, and 9) are illustrated in Figure 2. XRD findings showed the decrease of crystalline size with increasing B_4C content in the Al-4Mg matrix that was studied to study the effects of B_4C on the Al-4Mg matrix via XRD analysis. Structural changes were also evident in the composite with increasing B_4C content through the disappearance of peaks and broadening of other peaks. From this observation, it can be inferred that the diffraction peaks are subject to change due to the composite's composition and the fabrication process employed. Upon the increment of B_4C content, the peaks exhibit a narrowing phenomenon, signifying the growth of particles within the metal matrix composite. The emergence of Al_3Mg_2, in conjunction with Al and B_4C, is evidenced in the Al-4Mg-xB_4C compositions [13]. Absolute crystal size variations observed for the various compositions have been quantitatively analyzed using classical Scherrer equation for the aluminum reflection peak. Structural presence of only Al, B_4C, and Al_3Mg_2 phases shows that the 560°C solid-state thermal energy was insufficient to initiate interfacial reaction phases such as Al_3BC or AlB_2, which occur above 650°C. The clear phase contrast of the dark angular B_4C particles from the bright Al-Mg matrix observed under SEM micrographs provided adequate distribution evidence, negating any further EDS analysis. The micro porosity was restricted to fine 1-10 mu range, confirming 94% relative density stability for reinforcement content less than 6 wt.% and above 9 wt.% clustering becomes evident.

3.2. Hardness Analysis

The increased hardness in Al–Mg composites reinforced with B_4C is due to several intertwined strengthening mechanisms. The solid B_4C particles act as barriers to slip movement (Orowan mechanism) and contribute to improved load transfer from the soft matrix to the solid particles. The differences in the coefficient of thermal expansion between aluminum and B_4C also generate residual stresses and increase the slip intensity. Furthermore, the presence of the particles facilitates grain refinement according to the Hall–Petch relationship, leading to increased deformation resistance and a significant increase in hardness up to the optimum ratio (≈6%). However, when the ratio increases to 9%, the particles begin to agglomerate, increasing the likelihood of porosity and interfacial defects. This weakens the bond among the matrix and the

reinforcement, and the relative strengthening efficiency decreases. This explains the lower hardness compared to 6%, despite remaining higher than that of the base alloy [14-16]. For conformity to the ASTM E384 criteria and to balance out any microstructural differences within the local regions of the soft matrix and hard ceramics, at least 5 random indentations had to be taken on each sample. The results of these calculations showed standard deviations in scattering ranging from 3 HV to 6 HV. No error bars have been plotted in the graph for the sole purpose of maintaining clarity in the structure and focusing on mean value comparisons only.

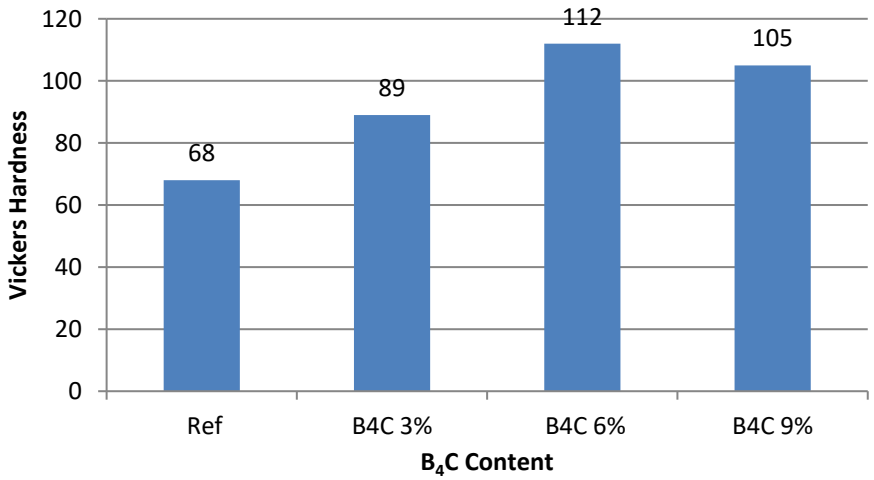

Fig. 3. Hardness test patterns of composites sintered of Al-4%Mg-XB_4C composites

3.3. Corrosion Resistance Analysis

Figure 4 shows the polarization curves for the base alloy Al-4Mg and its composite in a 3.5 weight percent NaCl solution. When varying amounts of B_4C were added, the Al-4Mg alloy's polarization behavior changed. The absence of a passive plateau on the Al-4Mg alloy's polarization curves is probably due to the selective dissolving that takes place around the Al_3Mg_2 phase. Introducing 3 wt.% of B_4C produced a negative effect on the corrosion potential (E_{corr}) and reduced the corrosion rate from 0.9812 to 0.02855 mm/yr. The addition of B_4C particle content helps reduce the current density of active sites upon the surface of material. The Al-4Mg-3B_4C sample showed pitting corrosion at a potential of (-737.5 mV) with an increase electrochemical potential; furthermore, the specimen demonstrated a pseudo-passive region

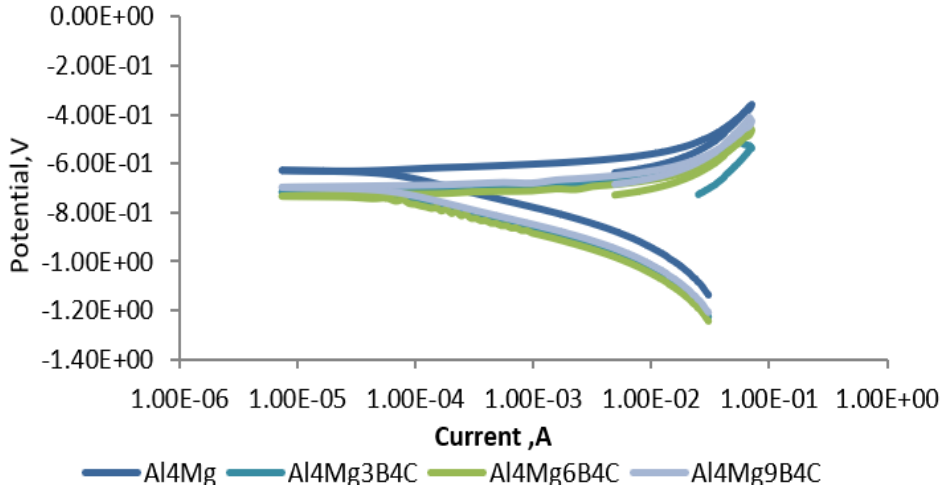

Fig. 4. Polarization curves of Al-4Mg/xB_4C (a) 0% (b) 3% (c) 6% (d) 9% composites in 3.5% NaCl solution

The incorporation of 6wt% B_4C into the Al-4Mg alloy specimen significantly reduced the corrosion rate to 0.01902 mm/yr, and no visible pitting corrosion was observed in the polarization curve. The incorporation of B_4C particle content may decrease the boundaries of the particles exposed to

the solution, thereby decreasing the rate of chemical corrosion. A reduction in the number of active sites is observed with an increase in the reinforcement content, specifically until reaching 6% B_4C. Introducing non-metallic particles appears to enhance the functionality of the alloy. It is hypothesized that the alloy surface possesses voids, spaces, and imperfections, and that B_4C particles may assist in occluding these, thereby mitigating the rate of metal dissolution. Up to a 9% reinforcement percentage, the composite's corrosion resistance is clearly improved. The higher corrosion resistance of the Al-3Mg alloy, which is made possible by the presence of non-metallic particles and the decrease in porosity in the microstructural composition, can be connected to the notable drop in the corrosion rate observed in the Al-3Mg-3B_4C and Al-3Mg-6B_4C composite.

Further addition of B_4C particle content increased the corrosion rate. Polarization curve for Al-3%Mg-9%B_4C composite appears to be similar to polarization curve of Al-3Mg alloy. The composite with 9% content of B_4C exhibits be slight increase in corrosion potential, whereas the cathodic current exhibits elevated values in comparison to the Al-3Mg alloy. The increased values of cathodic current can be elucidated by the increased of the B_4C particles content. The anodic current of polarization curve decreased by several orders of magnitude, an indication of susceptibility to localized forms of corrosion [17]. The corrosion rate observed for the sample containing 9 wt.% B_4C exhibited an increase, which was attributable to the development of pores within the agglomerated regions of B_4C, which consequently enhanced the ingress of the corrosive medium into the composite material. Furthermore, the elevation in the amount of exfoliated B_4C serves to activate the galvanic corrosion process of Al-3Mg, thereby contributing to an increased corrosion rate.

Table 2. Corrosion parameters of Al-4Mg/XB_4C composite in %3.5 NaCl solution

Samples	Ecorr. (mV)	Icorr. (μA)	βa (mV/decade)	βc (mV/decade)	CR (mmpy)	OCP (V)
Al-4Mg	-676	90.1	139.2	642.5	0.9812	-0.73632
Al-4Mg-3B_4C	-790	2.08	90.7	70.3	0.02855	-0.745026
Al-4Mg-6B_4C	-766	1.170	103.5	117.4	0.01902	-0.768087
Al-4Mg-9B_4C	-676	54.20	22.9	314.8	0.5109	-0.733673

The corrosion parameters of the composite samples and the basic Al-4Mg alloy in a 3.5 weight percent NaCl solution are displayed in Table 2. The Tafel extrapolation was used to calculate the corrosion potential and current density measurements. The tabulated data makes it abundantly evident that the incorporation of B_4C particles led to a reduction in the values of the corrosion current density (I_{corr}). According to earlier research, adding inert particles to a metallic substrate can improve the metal's resistance to corrosion because of the inert physical barrier function these particles provide [18]. As a result, the B_4C particles' influence has been shown to lower I_{corr} values. The impact of reinforcement on the corrosion resistance of aluminum alloys in a 0.05 M NaCl solution was examined in [18], who found that the polarization behavior of the alloys and composites was comparable. The authors added that depending on the particular alloy system, deaeration circumstances, and the method used to fabricate the composite, the addition of reinforcement may result in corrosion potential values that are more positive, more negative, or remain unchanged.

3.4. Cycling Polarization Analysis

Figure 5 illustrates the cyclic polarization behavior of Al-4Mg-xB_4C composites, to evaluate the pitting susceptibility of the composite. Analysis shows that the electrochemical potentials for the Al-4Mg, Al-4Mg-3B_4C, and Al-4Mg-6B_4C curves are more positive than that for the Al-4Mg-9B_4C curve. The cyclic polarization profile for Al-4Mg-6B_4C indicates the formation of a stable oxide layer on the surface of the composite, accompanied by the absence of a hysteresis loop. This finding suggests a commendable pitting resistance, indicating no likelihood of compromising the passivity of the surface [19]. According to the galvanic series, Mg possesses a more noble solution potential than the aluminum matrix. Consequently, regions with elevated Mg content function as cathodes, thereby inducing a potential difference at the interfaces. Moreover, the presence of Mg may have facilitated the formation of Al_4Mg, as it has been documented that intermetallic phase emerge at

the interfaces [20]. The electrochemical measurements have been made exclusively in 3.5 wt. % NaCl electrolyte to realistically represent the highly corrosive environment associated with chlorides. In order to ensure that electrochemical equilibrium was established and reliable statistics was provided, potentiodynamic scans were done in three replicates after the stabilization of the OCP stage. Corrosion rates (mm/yr) were quantitatively determined using the integrated Gamry software through Faraday's law by using the accurate linear Tafel extrapolation within a limited voltage window of 250mV relative to the open-circuit E_{corr}. Typical uncertainty associated with I_{corr} values ranged between 5% to 12%. The degradation process is essentially controlled by the kinetics of micro-galvanic cells that work at the interfaces between active aluminum matrix and secondary Al_3Mg_2 intermetallic precipitates instead of B4C non-conducting phases. The superior performance of 6 wt. % system is justified by the inert barrier properties that prevent Cl ions from penetration, combined with low porosity level. The lack of the anodic hysteresis loop during the cyclic polarization scan clearly indicates the superior performance of passive film, which is resistant to pitting and forms the barrier of the degraded product - $Al(OH)_3$.

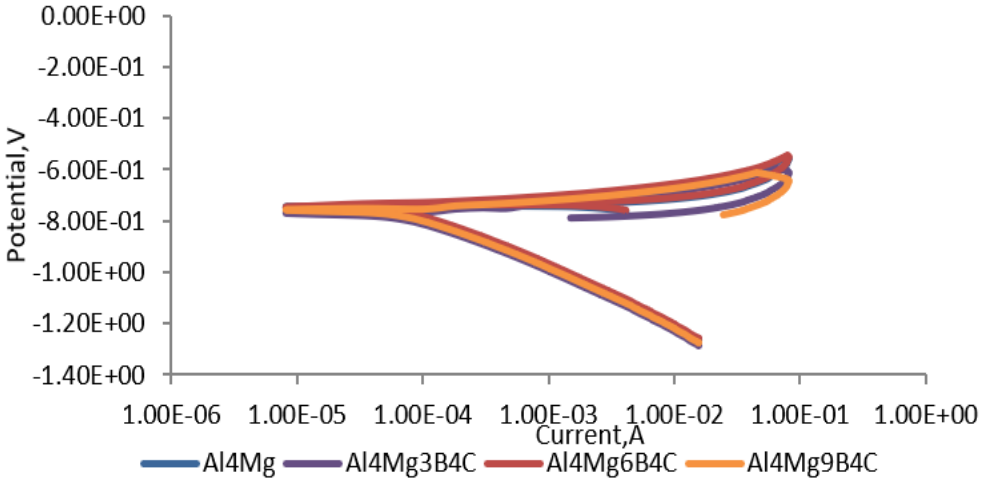

Fig. 5. In a solution containing 3.5 weight percent sodium chloride, the cyclic polarization graph of Al-4Mg alloy as well as Al-4Mg-XB_4C composites

3.5. Scanning Electron Microscope After Corrosion Test

Although adding magnesium to the alloy mix is essential for creating high strength alloys, it has been noted that this addition significantly reduces the corrosion resistance of aluminum alloys. Through a powder metallurgy process, magnesium particles are incorporated into the alloy's matrix phase, resulting in their concentration in a variety of second-phase particles. Additionally, the formation of Al-Mg intermetallic complexes speeds up the corrosion process by facilitating the cathodic reduction of oxygen [21]. Consequently, the passive coatings created on the Al-Mg intermetallic particles have different chemical characteristics and are less protective than those formed on the aluminum matrix. Aluminum's corrosion behavior is significantly impacted by the presence of magnesium intermetallic. The importance of intermetallic particles as possible corrosion beginning sites has been investigated by numerous other researchers [22]. Figure 6 shows the SEM micrographs of corroded samples for the Al-4Mg base alloy strengthened by B_4C particle concentration in the 3.5 weight percentage sodium chloride solution. Figure 6a illustrates the influence that the corrosion analysis had on the surface morphology of the specimen made of Al-4Mg alloy. It is evident that certain regions exhibit significant corrosion due to the presence of electrolytic ions. The micrograph reveals that the Al-4Mg alloy has been subjected to considerable degradation by the corrosive agents. The white particulates possess a substantial Mg concentration, suggesting that these particulates are intermetallic compounds of aluminum and Mg. The elemental composition of Al-4Mg alloy contains intermetallic precipitates like Al_3Mg, which increase the rate of corrosion in the alloy. Figure 6b illustrates the corroded specimen of the Al–4%Mg-3B_4C composite; it is observed that the incorporation of B_4C particle content within the Al-4Mg alloy leads to a reduction in uniform corrosion, while simultaneously inducing a localized pitting corrosion effect on the surface. The inclusion of B_4C particles serves to mitigate the

environmental assaults on the surfaces. Consequently, a diminished passage of electrolyte ions through the surface results in a decrease in the corrosion current values. It was observed that pitting corrosion disappeared with increasing B_4C particle content of the composites, while the uniform corrosion increased. Figure 6c portrays the corroded Al-4%Mg-9%B_4C specimen, which stands out with the highest level of corrosion resistance against all other samples. It is evident that the incorporation of B_4C and Mg particles within the Al-4%Mg-9%B_4C specimen confers optimal protective efficacy against environmental aggressors targeting the specimen. The sample in Figure 5d makes it clear that the composites were experiencing material surface deterioration. One especially interesting finding is that preferred dissolution appears to have an impact on Figure 6d. This result can be explained by the reinforcing phase's higher nobility as compared to the Al-4Mg alloy.

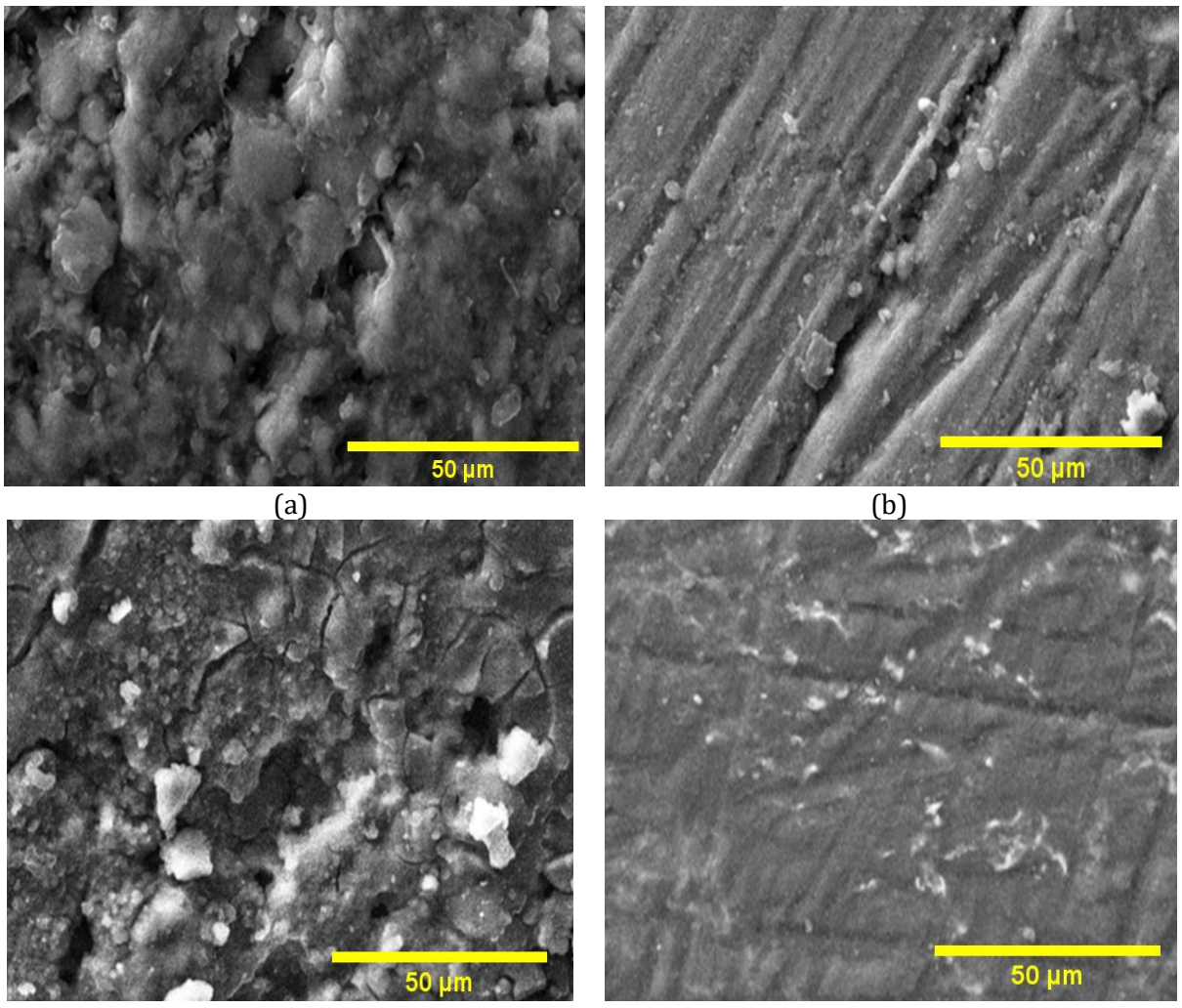

(a) (b)

(c) (d)

Fig. 6. SEM micrograph of corroded surface of (a) Al-4Mg alloy (b) Al-4%Mg-3B4C (c) Al-4%Mg-6B4C (d) Al-4%Mg-9B4C after polarization in 3.5 wt% NaCl solution

The significant presence of oxygen in areas of the matrix next to the reinforcement may lead to additional hypotheses on the galvanic impact that exists within the matrix as well as the reinforcement. Except for the Al-4Mg-6B_4C composite, which shows pitting corrosion that gets worse as the amount of B_4C particles increases, the main corrosion mechanism seen in the alloy with reinforcement within a 3.5% NaCl solution is both uniform corrosion and galvanic corrosion. This is because the intermetallic phase's electrochemical potential difference in the matrix helps to reduce the likelihood of pit corrosion in the composites [23]. Aluminum-based composites are prone to localized corrosion; multiple investigations on the corrosion behavior of aluminum along with its composites in chloride-filled environments have shown that the microstructural characteristics of the alloy and its composition play a major role in the initiation of localized

deterioration (which are then influenced by the processing methods used). Micro-galvanic coupling among the matrix and the reinforcement or among the matrix and intermetallic phases, disruption of the protective oxide layer as a result of micro-segregation of alloying constituents, or the existence of micro-crevices at the interface between the matrix and reinforcement are examples of potential mechanisms.

4. Conclusions

In this experiment, the development of Al-Mg matrix-based composite materials containing varying wt.% (0, 3, 6, and 9 wt.%) of micro B_4C particles was successfully achieved through cold compaction under 100 MPa and solid-state sintering in vacuum at 560°C. The process was highly successful in creating the composites that exhibited low porosity (1-10 μm) and very high relative densities of between 92% and 96%, especially in composite specimens having reinforcing fractions up to 6 wt.%. The solid-state sintering was carried out in order to avoid any risk of liquefaction of the matrix and formation of brittle reaction phases such as Al_3BC or AlB_2, thus maintaining the structural integrity of the phases. The particulate phase of B_4C showed an excellent spatially homogeneous distribution up to 6 wt.% while increasing the B_4C loading to 9 wt.% resulted in clustering and agglomeration of B_4C particles and hence caused the development of micro porosity in the material. As far as the mechanical behavior is concerned, the Vickers hardness of the alloy increased linearly with increase in B_4C percentage up to 9 wt.%. This is as a result of the interaction between the effects of grain refinement, verified through Scherrer crystallite size reduction, and the Orowan strengthening mechanism due to dispersion of hard ceramic particulate that inhibits dislocation movements. In addition, potentiodynamic polarization and cyclic polarization analysis done in the usual 3.5% NaCl solution indicated that the 6% B_4C composite is the best threshold when it comes to resisting corrosion since it has the lowest Icorr and corrosion rate. The B_4C particles dispersed uniformly serve as an excellent physical barrier which effectively impedes the diffusion of aggressive chloride ions. Moreover, the absence of the anodic hysteresis loop in the cyclic polarization study for the 6 wt.% composite confirms its ultimate passive film stability and resistance against localized pitting corrosion. On the other hand, the corrosion resistance was significantly reduced when B_4C content reached 9 wt.%, as the agglomeration of the particles and high micro-porosity served as sites for entrapment of the electrolytes causing the micro-galvanic cells to operate in the interface of the matrix and intermetallic Al_3Mg_2 particles. In general, the Al-Mg 6 wt.% B_4C composite presents a good configuration, since it gives rise to an improved hardness performance, as well as excellent passivity against corrosion, thus being a very promising material for marine engineering applications.

Acknowledgement

The authors thank the University of Kufa, University of Mustansiriyah for providing laboratory support.

References

[1] Azaath LM, Natarajan U, Veerappan G, et al. Experimental investigations on the mechanical properties, microstructure and corrosion effect of Cu-20Al-4Ni/SiC composites synthesized using powder metallurgy route. Silicon, 2022; 14: 5993-6002. https://doi.org/10.1007/s12633-021-01363-2

[2] Duraipandian, Mummoorthi. Effects of Fe2O3 and B4C addition on the mechanical properties and corrosion resistance of Al-Mg-Si Alloy in 3.5% brine solution. Metals and Materials International, 2021, 27.6: 1506-1518. https://doi.org/10.1007/s12540-019-00548-0

[3] Singh I, Mandal D, Singh M, Das S. Influence of SiC particles addition on the corrosion behavior of 2014 Al-Cu alloy in 3.5% NaCl solution. Corrosion Science, 2009; 51: 234-241. https://doi.org/10.1016/j.corsci.2008.11.001

[4] Gao Y, Qiu F, Liu T, Chu J, Zhao Q, Jiang Q. Effects of carbon source on TiC particles distribution, tensile, and abrasive wear properties of in situ TiC/Al-Cu nanocomposites prepared in the Al-Ti-C system. Nanomaterials, 2018; 8: 610. https://doi.org/10.3390/nano8080610

[5] Kumar N, Sharma A, Manoj MK. Influence of different aqueous media on the corrosion behavior of B4C-modified lightweight Al-Mg-Si matrix composites. Materials, 2022; 15: 8531. https://doi.org/10.3390/ma15238531

[6] Rahmani K, Majzoobi GH, Ebrahim-Zadeh G, Kashfi M. Comprehensive study on quasi-static and dynamic mechanical properties and wear behavior of Mg-B4C composite compacted at several loading rates through powder metallurgy. Transactions of Nonferrous Metals Society of China, 2021; 31: 371-381. https://doi.org/10.1016/S1003-6326(21)65502-4
[7] Ghalib L, Mahdi SM, Majeed AH. Hardness and corrosion behavior of Al-Ti-Cu alloys fabricated by powder metallurgy technique. Emergent Materials, 2024; 7: 1191-1201. https://doi.org/10.1007/s42247-024-00665-6
[8] Jiang B, Xu S, Xu H, Hu M, He Y, Ji Z. Effect of Mg addition on microstructure and mechanical properties of Al-Si-Cu-Fe alloy with squeeze casting. Materials Research Express, 2019; 7: 016511. https://doi.org/1088/2053-1591/ab5cc6
[9] ASTM International. Standard Test Method for Conducting Potentiodynamic Polarization Resistance Measurements. ASTM G59-97(2014). ASTM International, 2014.
[10] ASTM International. Standard Practice for Calculation of Corrosion Rates and Related Information from Electrochemical Measurements. ASTM G102-89(2004). ASTM International, 2004.
[11] Karakulak E, Yamanoğlu R, Erten U, Zeren A, Zor S, Zeren M. Investigation of corrosion and mechanical properties of Al-Cu-SiC-xNi composite alloys. Materials & Design, 2014; 59: 33-37. https://doi.org/10.1016/j.matdes.2014.02.039
[12] Kumar N, Gautam A, Singh RS, Manoj MK. Study of B4C/Al-Mg-Si composites as highly hard and corrosion-resistant materials for industrial applications. Transactions of the Indian Institute of Metals, 2019; 72: 2495-2501. https://doi.org/10.1007/s12666-019-01717-w
[13] Ghandvar H, Jabbar MA, Koloor SSR, Petrů M, Bahador A, Bakar TAA, Kondoh K. Role of B4C addition on microstructure, mechanical, and wear characteristics of Al-20%Mg2Si hybrid metal matrix composite. Applied Sciences, 2021; 11: 3047. https://doi.org/10.3390/app11073047
[14] Kumar TK, Kandavel A. Mechanical characterization of B4C-GR reinforced Al-Zn-Mg alloy hybrid nanocomposites. Materials Transactions, 2023; 64: 955-961. https://doi.org/10.2320/matertrans.MT-M2022168
[15] Gök DA, Bayraktar C, Hoşkun M. A review on processing, mechanical and wear properties of Al matrix composites reinforced with Al2O3, SiC, B4C and MgO by powder metallurgy method. Journal of Materials Research and Technology, 2024; 31: 1132-1150. https://doi.org/10.1016/j.jmrt.2024.06.110
[16] Ananiadis, Elias A., et al. Aluminium matrix composites reinforced with AlCrFeMnNi HEA particulates: Microstructure, mechanical and corrosion properties. Materials, 2023, 16.15: 5491. https://doi.org/10.3390/ma16155491
[17] Toptan F, Alves A, Kerti I, Ariza E, Rocha L. Corrosion and tribocorrosion behaviour of Al-Si-Cu-Mg alloy and its composites reinforced with B4C particles in 0.05 M NaCl solution. Wear, 2013; 306: 27-35. https://doi.org/10.1016/j.wear.2013.06.026
[18] Majed RA, Mahdi M, Al-Kaisy HA, Maged SAA. Corrosion behavior for Al-Cu-Mg alloy by addition SiO2 particles in seawater. Engineering and Technology Journal, 2014; 32: 354-364. https://doi.org/10.30684/etj.32.2A.6
[19] Dikici B, Bedir F, Gavgali M. The effect of high TiC particle content on the tensile cracking and corrosion behavior of Al-5Cu matrix composites. Journal of Composite Materials, 2020; 54: 1681-1690. https://doi.org/10.1177/0021998319884098
[20] Blanc C, Freulon A, Lafont M, Kihn Y, Mankowski G. Modelling the corrosion behaviour of Al2CuMg coarse particles in copper-rich aluminium alloys. Corrosion Science, 2006; 48: 3838-3851. https://doi.org/10.1016/j.corsci.2006.01.012
[21] Mayyas AT, Hamasha MM, Alrashdan A, Hassan AM, Hayajneh MT. Effect of copper and silicon carbide content on the corrosion resistance of Al-Mg alloys in acidic and alkaline solutions. Journal of Minerals and Materials Characterization and Engineering, 2012; 11: 335-352. https://doi.org/10.4236/jmmce.2012.114025
[22] Ananiadis E, Argyris KT, Matikas TE, Sfikas AK, Karantzalis AE. Microstructure and corrosion performance of aluminium matrix composites reinforced with refractory high-entropy alloy particulates. Applied Sciences, 2021; 11: 1300. https://doi.org/10.3390/app11031300
[23] Wang J, Zhu R, Liu Y, Zhang L. Understanding melt pool characteristics in laser powder bed fusion: An overview of single- and multi-track melt pools for process optimization. Advanced Powder Materials, 2023; 2: 100137. https://doi.org/10.1016/j.apmate.2023.100137